Metal-Mediated Peptide Ion Conformations in the Gas Phase

John A. Taraszka, Jianwei Li, and David E. Clemmer*

Department of Chemistry, Indiana University, Bloomington, Indiana 47405

Received: November 8, 1999; In Final Form: February 24, 2000

The influence of metal cations and source temperature on the conformations of oxidized insulin chain A (ICA) anions has been investigated in the gas phase by high-resolution ion mobility techniques. Cross sections for non-metalated $[ICA\text{-}nH]^{n-}$ ($n = 2-6$) ions show a distinct Coulomb-driven unfolding transition when four or more protons are removed. Studies of $[ICA\text{-}6H + M^{2+}]^{4-}$ ions (where M = Ca, Mn, Co, Ni, Cu, or Zn) show that metal peptide ions favor specific types of conformations that depend upon the binding properties of the metal. Doubly-charged metal ions appear to bind to multiple sites (presumably through interactions with $-SO_3^-$, $-COO^-$, and amide groups on various amino acids) and have a pronounced effect on the number and shapes of stable conformations. Generally, $[ICA\text{-}6H + M^{2+}]^{4-}$ ions are found to be more compact than their $[ICA\text{-}4H]^{4-}$ analogues. Studies of $[ICA\text{-}5H + Na^+]^{4-}$ ions show that addition of Na^+ to the ICA anion has little effect on the peptide structure. The relative stabilities of different conformations for different metal ions are discussed in terms of simple qualitative potential energy surfaces.

Introduction

Metal ions play key roles in many biological processes, including establishment of macromolecular structure, storage and transfer of electrons, small molecule binding, and catalytic activity.[1] Recent advances in ion sources[2,3] for mass spectrometry (MS) have made determination of the number and identity of metals bound to a range of biomolecules routine for many types of systems. A number of research groups have investigated the fragmentation of metalated peptides,[4] oligonucleotides,[5] and oligosaccharides.[6,7] In some cases, it appears that new pathways arise when metals are present.[4a,b,f,i] Selective binding of metals to oligomers that induce favorable fragmentation patterns could have an impact on sequencing strategies. As a first step in addressing selectivity, it is important to understand the general nature of the metal−peptide precursor ion complex. Several studies of protein fragmentation have shown that fragment peaks are influenced by the conformation of the gas-phase protein ion prior to activation.[8] Other studies indicate that observed fragments depend on the chemical properties of the bound metal ion and the sequence and length of the peptide.[4c−i] In general, fragmentation data provide information about the nature of the dissociative transition state; currently, little is known about the influence of the metal ion on low-lying states of the metal−peptide ion conformation in the gas phase.

In this paper, we report high-resolution ion mobility studies of the conformations of insulin chain A (ICA) anions bound to a range of metal cations (Na^+, Ca^{2+}, Mn^{2+}, Co^{2+}, Ni^{2+}, Cu^{2+}, and Zn^{2+}). To our knowledge, no similar solution-phase experiments with ICA have been reported. Our long-term goal in these studies is to provide detailed structural information about binding in the absence of solvation effects. However, the data we have obtained (even for binding to a relatively small 21 residue peptide) indicates that these systems are very complex. Here we report what is largely a qualitative description of the general features observed. We focus on metal−peptide complexes having a net charge of −4, where repulsive Coulombic forces (that favor elongated structures) are nearly balanced with attractive charge-solvation, hydrogen-bonding, and van der Waals interactions (that favor compact globular conformations). Transition metals appear to bind in multiple distinct configurations leading to specific metal−peptide ion conformations. The stabilities of these states are highly influenced by specific metal−ligand (M−L) binding interactions, and thus are mediated by the metal.

The present work is related to recent ion mobility studies of the alkali metals bound to poly(ethylene glycol) and poly(ethylene terephthalate) carried out by Bowers and co-workers.[9,10] This group has performed studies as a function of drift tube temperature and determined an activation barrier of 1.6 kcal mol^{-1} for the isomerization of Na^+−poly(ethylene terephthalate)$_3$ from an open to closed form.[10] The same group also studied sodiated oligosaccharides[11] and peptides.[12] Hill and coworkers have also carried out studies of sodiated peptides where they concluded that Na^+ substituted for a proton.[13] In addition to fragmentation studies[4] and ion mobility measurements,[12−17] several other MS-based methods are currently being developed to examine the conformations of protein ions. These include measurements of collision cross sections in triple quadrupole instruments;[18] kinetic energy release measurements;[19] microscopy studies of surfaces bombarded with high-energy ions;[20] measurements of proton transfer reactivity;[21,22] measurements of gas-phase H−D exchange levels[22,23,24] and gas-phase basicities;[25] and studies of adduct formation.[26,27,28]

Experimental Section

General. ICA (oxidized bovine, Sigma 80%) is a 21-residue polypeptide (GIVEQCCASVCSLYQLENYCN), where the thiol groups on the cysteine residues (C) are oxidized to $-SO_3H$ groups. Ion mobility techniques[14] and their application to biomolecular ions have been discussed in detail previously.[15] The high-pressure high-resolution ion mobility mass spectrometer used here has also been described previously.[29] For the non-metalated peptide, a 4×10^{-4} M solution of ICA was prepared in 50:50 water:acetonitrile. Metal−peptide adducts were formed by adding a metal acetate salt (Na^+, Ca^{2+}, Mn^{2+}, Co^{2+}, Ni^{2+}, Cu^{2+}, or Zn^{2+}) at a metal ion concentration of 2×10^{-4} M to

10.1021/jp9939468 CCC: $19.00
Published on Web 04/01/2000

the 4×10^{-4} M ICA solution. Solutions were electrosprayed at atmospheric pressure into a differentially-pumped variable-temperature capillary source. Ions exit the source at high pressure (~200 Torr) and are guided to the drift tube under the influence of an electric field. A 150 μs pulse of ions is introduced into the drift region using a parallel wire ion gate similar to one described previously by Hill and co-workers.[14d] The drift region is 49.81 cm long and was operated at a pressure of ~250 Torr and an electric field strength of 200.8 V cm^{-1}. Some of the ions exit the drift tube through a 100 μm aperture, where they are focused into a quadrupole mass filter. The quadrupole can be scanned to obtain mass spectra or fixed to transmit a narrow *m*/*z* range for mobility measurements. Ions are detected with an off-axis collision dynode/microchannel plate detector.

Variable-Temperature ESI Source. The ESI capillary is encased in an aluminum block that can be heated with cartridge heaters. Temperatures are measured by a thermocouple that is mounted to the aluminum block. The temperature was calibrated to reflect the temperature of the flowing gas that exits the capillary in a series of separate experiments. We expect that the reported temperatures reflect the gas temperature to within ±5 K.

Cross Sections. Most of the ion mobility data are plotted on a cross section scale. This is done by converting drift times to cross sections by using[15]

$$\Omega = \frac{(18\pi)^{1/2}}{16}\frac{ze}{(k_B T)^{1/2}}\left(\frac{1}{m_I}+\frac{1}{m_{He}}\right)^{1/2}\frac{760ET}{273.2LPN}t_D \quad (1)$$

where t_D is the drift time, E is the electric field strength in the drift tube, L is the length of the drift tube, P is the buffer gas pressure, z is the charge state, N is the neutral number density, T is the drift tube temperature, k_B is Boltzmann's constant, e is the charge of an electron, and m_I and m_{He} are the masses of insulin chain A and helium, respectively. In addition, it is necessary to correct for the flight times of ions in other parts of the instrument as well as the ions' energies at the exit of the drift tube in the presence and absence of buffer gas. This correction is small (~150−250 μs) in these experiments.

Molecular Modeling and Cross Section Calculations for Trial Structures. Molecular mechanics and dynamics were performed using the extensible systematic force field (ESFF) on Biosym's Discover 3.0.0 software.[30] One hundred energy-minimized trial conformations were generated through a simulated annealing protocol in which ions were heated to 1000 K for 2 ps and then cooled to 300 K over 1 ps. Collision cross sections for energy-minimized trial conformations were estimated by determining the orientationally averaged projection using a method that is analogous to those previously discussed.[9] This method treats the interactions between atoms of the biomolecule and the buffer gas as hard-sphere collisions and assumes a rigid trial conformation. This method does not include a term for the scattering of the buffer gas; it is generally believed to provide a lower limit to the true collision integral, which can be more accurately calculated using more intensive calculations.[31] For the present study we use this approach only to gain a qualitative understanding of the sizes of different conformations.

Results and Discussion

Non-metalated ICA Ions. In order to understand the influence of each metal ion on conformation it is instructive to examine the non-metalated peptide system. Figure 1a shows

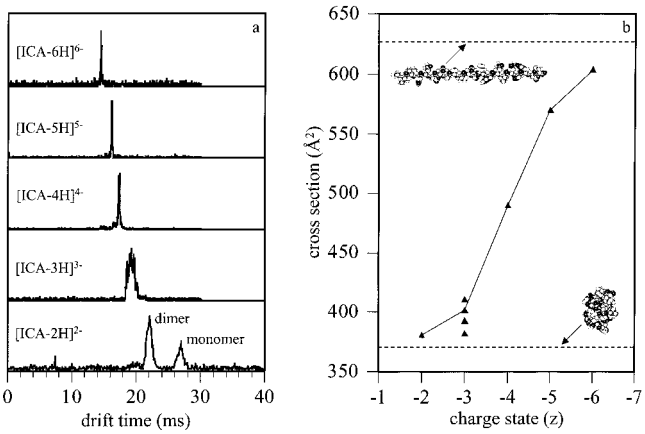

Figure 1. (a) Ion mobility distributions for the −2 to −6 charge states of non-metalated insulin chain A ions formed by electrospray ionization. These distributions have been normalized to a buffer gas pressure of 250.0 Torr and a drift field of 200.8 V cm^{-1}. The two peaks in the −2 charge state distribution labeled dimer (~22 ms) and monomer (~27 ms) were assigned based on comparisons with calculated trial structures. See text for details. (b) Cross sections as a function of deprotonation state for the main features associated with the monomer −2 to −6 charge states as determined from the data in part a and eq 1. The dashed lines denote calculated cross sections for a highly compact state created by molecular modeling and a near-linear conformation (as shown by the space-filled models). The solid line passes through the most intense feature of the distribution of the −3 charge state. See text for details.

drift time distributions for the −2 to −6 deprotonation charge states of ICA. As the ion charge state increases, the measured drift time decreases. This occurs because the drift force increases. The −2 charge state shows two peaks. Using eq 1 (and assuming that only $[ICA\text{-}2H]^{2-}$ ions are present) we determine cross sections of 316 and 381 Å^2 for the ions corresponding to the peaks at 22 and 27 ms, respectively. The former value is much smaller than the calculated cross section (Ω = 370 Å^2) for a very compact conformation of the $[ICA\text{-}2H]^{2-}$ ion generated by molecular modeling. We assign this peak to a multiply-charged $[ICA_2\text{-}4H]^{4-}$ dimer (having a *m*/*z* ratio that is the same as the $[ICA\text{-}2H]^{2-}$ monomer). The mobilities of multiply-charged dimers are typically higher than monomers (having the same *m*/*z* ratios) because the former ions experience twice the drift force, whereas the cross section increase is less than a factor of 2 (~$2^{2/3}$ for geometries that are roughly spherical). Multiply-charged ESI multimers, having the same *m*/*z* value as an expected monomer charge state, have been observed by a number of groups.[32,33] The present assignment is consistent with a stability model for aggregates that we developed previously; multimers are not observed for higher charge states because noncovalent (weak) interactions are unable to stabilize the stronger repulsive coulomb force.[32] Peaks for the −4 to −6 ions are substantially narrower than those for lower charge states. Comparison of these peak shapes with the calculated peak shape for transport of a single ion conformation[34] shows that even very sharp peaks are broader than the distribution calculated for a single conformation. This indicates that multiple unresolved states or conformers that interconvert over the experimental time scale are present for all charge states. There are at least four reproducible maxima in the −3 distribution, indicating that at least four conformations are stable.

Figure 1b shows a plot of cross sections for the main features in the drift time distributions (part a) for the different charge states. Comparison of these values with calculated cross sections for a limiting linear structure and an extremely compact conformer generated by molecular modeling shows that the shapes of ICA ions vary substantially depending upon the charge

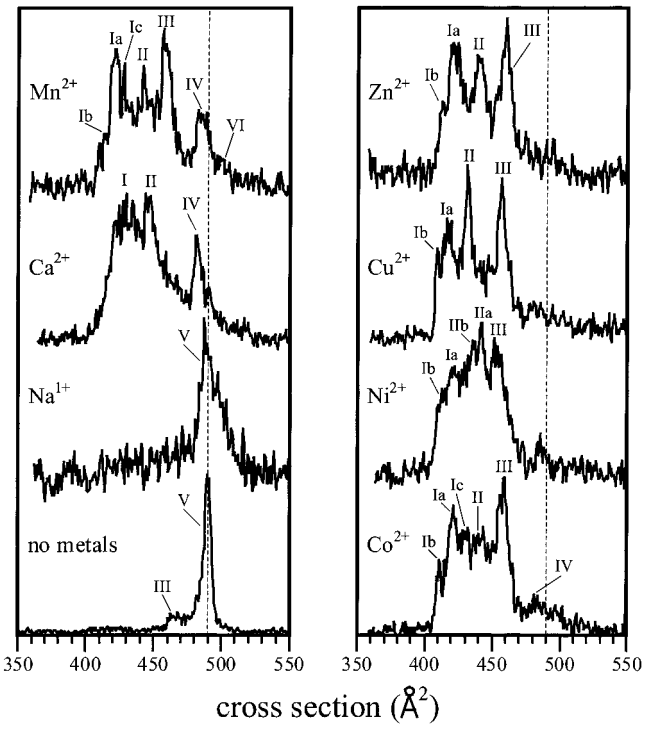

Figure 2. Cross section distributions determined from ion mobility data for the $[ICA\text{-}4H]^{4-}$, $[ICA\text{-}5H + Na^{+}]^{4-}$, and $[ICA\text{-}6H + M^{2+}]^{4-}$ (M = Ca, Mn, Co, Ni, Cu, and Zn, as labeled) ions at a source temperature of 300 K. The dashed line corresponds to the cross section of the $[ICA\text{-}4H]^{4-}$ ion and is used as a reference throughout. Roman numeral (and arabic) assignments of peaks are described in the text.

state. A distinct unfolding transition is observed when four or more protons are removed. The transition from compact to elongated structures with increasing charge state can be explained by a Coulomb-induced unfolding transition; this behavior has been discussed extensively for larger protein systems.[16−18a,b] The large 605 Å^2 cross section for the −6 state is near the 628 Å^2 calculated limit for a linear conformation obtained through molecular modeling, indicating that this ion has a nearly linear geometry. The −5 cross section (562 Å^2) is somewhat smaller, indicating that some elements of secondary structure exist. We rule out structures arising from folding in the middle of the peptide where the C-terminal and N-terminal ends are in close proximity because the calculated cross sections for these types of geometries are far below the experimental measurements. Highly-extended conformations are favored because of the relatively large Coulomb repulsion associated with the high density of deprotonated sites on the relatively short (21 residue) polypeptide chain.

Ion Mobility Peak Nomenclature for Metalated ICA Ions. Metalated peptides exhibit a complex distribution of peaks. Six major conformer types are discussed below and are denoted conformation I, corresponding to cross sections from 410 to 430 Å^2; II, 430 to 450 Å^2; III, 450 to 470 Å^2; IV, 470 to 485 Å^2; V, 485 to 495 Å^2; and VI, >495 Å^2. Multiple features within a conformation type are indicated by addition of "a" to indicate the most intense peak, "b" to indicate a reproducible feature to the left of the most intense peak, and "c" to indicate a feature to the right of the most intense peak. These labels for ion cross sections do not imply that structures with similar cross sections have similar binding interactions or structure, since differently folded structures could have similar cross sections.

Ion Mobility Distributions at 300 K. Figure 2 shows cross section distributions obtained at a source temperature of 300 K for the metalated and non-metalated −4 charge states. A wide range of structures for different metals is observed. The cross section distribution for $[ICA\text{-}5H + Na^{+}]^{4-}$ is dominated by a type V conformation similar to the data for the non-metalated $[ICA\text{-}4H]^{4-}$ ion; however, the fwhm of the peak corresponding to the sodiated peptide is 2.5 times broader than peak corresponding to the non-metalated peptide. All of the $[ICA\text{-}6H + M^{2+}]^{4-}$ ions exhibit a range of more compact conformers, having cross sections of ∼400−460 Å^2. The $[ICA\text{-}6H + Ca^{2+}]^{4-}$ distribution shows a broad feature corresponding to type I conformations and a partially resolved type II structure; a less intense type IV state is centered at Ω = 480 Å^2. While manganese data appear similar to those for calcium, the Mn^{2+} ion appears to stabilize many distinct conformations (Ib, Ia, II, and III). These conformers appear to be common to all of the transition metal complexes (Co, Ni, Cu, and Zn) studied here. The similarities between transition metal systems provide evidence that some conformations appear to be general types that are accessible in all transition metal systems. The abundances of the different states between the metal systems are reproducibly different, indicating that the ability of each metal to stabilize a specific conformer type is influenced by the specific binding interactions associated with each metal.

Relative Stabilities of Conformations. Some insight regarding the relative stabilities of different conformers can be obtained by performing studies at various source temperatures. Figure 3 shows cross section distributions obtained at capillary temperatures of 300, 350, and 390 K. Cross section distributions for $[ICA\text{-}4H]^{4-}$ and $[ICA\text{-}5H + Na^{+}]^{4-}$ ions do not change substantially over this range of temperatures. An intense type V conformer is favored at all temperatures, suggesting that this state is thermodynamically favorable for the non-metalated and sodiated peptides.

All of the $[ICA\text{-}6H + M^{2+}]^{4-}$ systems exhibit unfolding transitions with increasing source temperature. This indicates that the compact type I, II, and III conformers are relatively unstable for this charge state. Variations between different metal systems as a function of temperature may provide an indication of the strength of specific metal−ligand interactions. At 350 K the Ni distribution changes significantly—peaks corresponding to conformation types I and II are substantially smaller than at 300 K. At 350 K the most intense peaks correspond to conformation types IIIb and IIIa. The peak intensities for some other systems (Ca, Co, and Cu) change slightly at 350 K; however, these changes are small in all systems except those containing Ni.

At 390 K, significant changes are observed in the cross section distribution for all of the M^{2+} complexes. Each metal peptide system now displays a unique distribution of conformers. This indicates that each metal differs in its ability to stabilize different structures. The calcium ion principally unfolds to a type IV conformation while the Mn system unfolds to both type III and type IV conformers. The Co and the Ni systems display very similar distributions of type IIIa, IIIb, and IIIc conformations; however, the nickel system appears to effectively select for a new (type VI) conformation with a large cross section. The Co, Cu, and Zn distributions appear to select for type III conformers. Co and Cu also show a range of partially resolved type IV, V, and VI conformers; the type IV conformer is favored in the Cu system. The Zn system does not readily unfold to type IV, V, and VI conformers; only a small peak corresponding to a type IV conformation and a small broad peak corresponding to a type VI conformation are present.

General Trends among $[ICA\text{-}6H + M^{2+}]^{4-}$ Ions. A striking feature of these systems is the large number of different stable

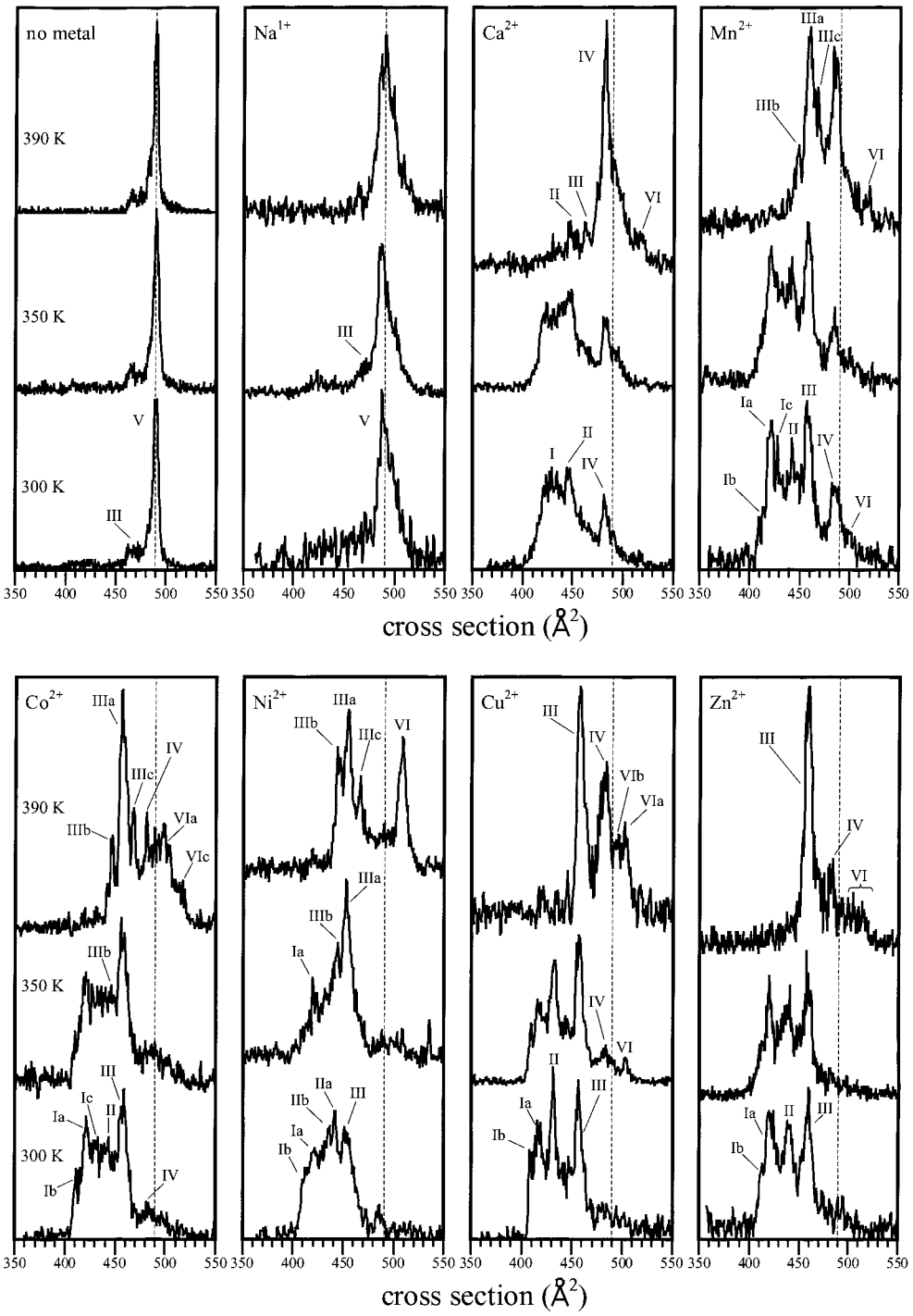

Figure 3. (a, top) Cross section distributions for $[ICA\text{-}4H]^{4-}$, $[ICA\text{-}5H + Na^+]^{4-}$, $[ICA\text{-}6H + Ca^{2+}]^{4-}$, and $[ICA\text{-}6H + Mn^{2+}]^{4-}$ ions at capillary temperatures of 300, 350, and 390 K, as indicated. (b, bottom) Cross section distributions for $[ICA\text{-}6H + Co^{2+}]^{4-}$, $[ICA\text{-}6H + Ni^{2+}]^{4-}$, $[ICA\text{-}6H + Cu^{2+}]^{4-}$, and $[ICA\text{-}6H + Zn^{2+}]^{4-}$ ions at capillary temperatures of 300, 350, and 390 K, as indicated. The dashed lines at 490 Å^2 denote the cross section of the $[ICA\text{-}4H]^{4-}$ ion.

conformations that are observed for the transition metal complexes. When multiple source temperatures are considered, 6−10 stable conformation states exist for the each of the transition metal systems. This is a rather dramatic contrast to the non-metalated and sodiated peptides where a single conformation type dominates under all source conditions. The difference in behavior between transition metal and sodiated systems can be partially rationalized by the differences in the metal binding interactions. The ability of transition metals to establish localized M−L bonds appears to be critical to stabilizing all compact states. We speculate that the multitude of different conformers arises from interaction of the M^{2+} metals with different combinations of ligands on the peptide. Possible ligands include $-COO^-$ groups on Glu and the C-terminus, $-SO_3^-$ groups on the oxidized Cys, and amide groups on the Asn and Gln amino acids. The many different stable conformations suggest that the metal may coordinate differently (number, geometry, and ligands) in each of the conformations.

Figure 4 shows a plot of the cross sections for the major conformation types observed for the metals at 300, 350, and 390 K. It is interesting that the type V conformation is only a major feature in the non-metalated and sodiated peptides. Apparently, addition of any +2 metal is sufficient to prevent formation of this state. At 300 K, type I and II conformations

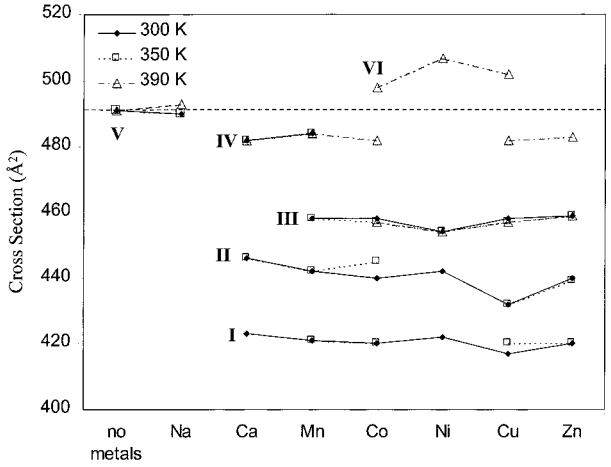

Figure 4. Major conformation types observed for metal ICA adducts at source temperatures of 300, 350, and 390 K. The horizontal dashed line at 490 Å^2 indicates the cross section of the $[ICA\text{-}4H]^{4-}$ ion.

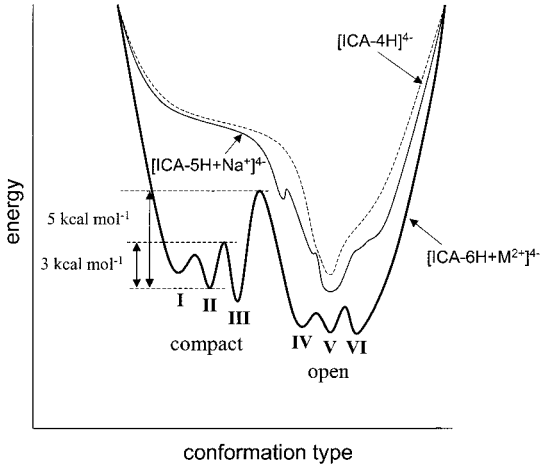

Figure 5. Qualitative potential energy sketches for different conformations of non-metalated $[ICA\text{-}4H]^{4-}$ (short dashed line), $[ICA\text{-}5H + Na^+]^{4-}$ (solid line), and metalated $[ICA\text{-}6H + M^{2+}]^{4-}$ (where M corresponds to one of the transition metal ions studied) ions (bold line). Activation energy estimates are described in the text for the I,II → III transition determined from the Ni system and the I,II → IV transition determined from the Ca system.

are observed for all of the M^{2+} complexes. Transition metals also form the type III state, while Ca^{2+} apparently cannot stabilize this state. This interesting difference suggests that the ability of transition metals to coordinate ligands is required for stabilization of the type III conformation. Although at 300 K the type IV conformer is only observed for Ca and Mn, this state does appear to be present for other metals at 390 K, as is especially apparent for Co, Cu, and Zn. The type VI conformation is observed only at high temperatures (390 K) for the later Co, Ni, and Cu metals. The overall similarities in cross sections for the type I, II, and III conformers among the different metal−peptide systems (at various temperatures) suggest M−L binding interactions that are required to stabilize these compact structures are accessible to all of the transition metal ions. Presumably, these involve the interaction of M^{2+} with multiple ligands. The specific orbital configuration of the metals may be more important for formation of some states. For example, it appears that Co, Ni, and Cu preferentially form type VI conformations (compared with other metals such as Zn).

Qualitative Potential Energy Surfaces for Conformations of $[ICA\text{-}4H]^{4-}$, $[ICA\text{-}5H + Na^+]^{4-}$, and $[ICA\text{-}6H + M^{2+}]^{4-}$ Ions. The structural transitions observed upon increasing the source temperature provide some insight into the relative stability of different conformers and folding/unfolding pathways. Upon leaving the heated capillary, ions enter the cool 300 K buffer gas where they drift under the influence of weak electric fields before entering the drift tube. This heating/cooling cycle is similar to the injected-ion method of annealing structures.[35] We expect metastable structures from the source (perhaps solution-like structure, retained during the ESI drying process) to anneal into energetically favorable gas-phase states upon exposure to the high-temperature capillary conditions.

For the Ca and Ni systems, we have estimated upper limits to activation barriers for transitions between compact (types I and II) conformations and more open type IV and III conformations, respectively. We calculate that under the flow conditions used, ions spend a minimum of 100 μs in the capillary.[36] Assuming a unimolecular unfolding transition from a compact to a more open conformation [and that the only conformations that exist initially (at 300 K) are types I and II (compact)], we obtain rough estimates of rate constants and activation energies for the unfolding process. Rate constants for the I,II → IV transition for $[ICA\text{-}6H + Ca^{2+}]^{4-}$ ion were estimated to be 2.6 × 10^{-3}, 4.4 × 10^{-3}, and 20.0 × 10^{-3} molecules s^{-1} at temperatures of 300, 350, and 390 K, respectively; from these, we estimate an upper limit to the activation barrier of 6 kcal mol^{-1}.[37] Similarly, rate constants for I,II → III transition for the Ni system were estimated to be 4.0 × 10^{-3} and 8.8 × 10^{-3} molecules s^{-1} at 300 and 350 K, respectively; thus the upper value for the activation energy is 3 kcal mol^{-1}. These upper limits are slightly larger than the 1.6 kcal mol^{-1} activation energy measured for the transitions in the smaller Na^+−poly(ethylene terephthalate)$_3$ system.[10]

Although we do not know the actual structures or absolute energies of these systems, we have attempted to generalize the trends that are observed by drawing a very simple (and highly speculative) potential energy diagram. Figure 5 shows qualitative potential energy surfaces that are consistent with our experimental results. Experimentally, we observe one dominant peak that is too wide to correspond to a single conformation for the $[ICA\text{-}4H]^{4-}$ ion. These data suggest that it is unlikely that vastly different conformation types (e.g., very compact or elongated forms) are populated significantly; however, the peak width is wider than expected for a single conformer, indicating that multiple structures are present. It is likely that these are related conformers that interconvert rapidly. We have drawn a potential surface with a minimum associated with the type V conformer with few barriers or deep wells that would trap other states (Figure 5). Substitution of a single Na^+ for a proton in this system appears to be a relatively minor perturbation of the $[ICA\text{-}4H]^{4-}$ surface. However, the peak corresponding to the type V conformer is ∼2.5 times broader than that of the $[ICA\text{-}4H]^{4-}$ ion. This suggests that at least a few conformations are somewhat more stable when Na^+ is attached (as indicated by the small wells in Figure 5). There is no evidence for a dramatic change in the stability of different states (relative to the non-metalated state).

The substantial change in behavior of the M^{2+} systems indicates that the relative stabilities of different conformations are markedly influenced by the addition of these metals. The presence of multiple peaks for $[ICA\text{-}6H + M^{2+}]^{4-}$ ions (having significantly smaller cross sections than the non-metalated ions) is evidence that M^{2+} ions stabilize compact conformers. The observation of resolved peaks in the ion mobility data requires that these conformers do not interconvert over the ∼20 ms experimental time scales at 300 K. Thus, substantial activation barriers between these states must exist. We have sketched a

series of wells that are lower in energy than the broad sloping non-metalated surface, which are consistent with the stabilities of these conformations.

Although there are similarities among the metal systems, variations in source temperatures show that there are also many differences. This indicates that well depths and barrier heights vary for different M^{2+} systems. The magnitude of these variations is difficult to assess from these data; however, several qualitative trends are apparent. The broad partially-resolved distributions, like those found in Ni and Co systems, suggest a more rapid interconversion (a relatively flat featureless surface) when compared to the sharp well-resolved peaks observed for the Cu and Zn distributions. This is evidence for a substantially rougher landscape for the Cu and Zn potential surfaces.

Figure 5 shows the location of activation energy estimates. The type I,II → III unfolding transition of the $[ICA\text{-}6H + Ni^{2+}]^{4-}$ ion occurs over an activation barrier of ~3 kcal mol^{-1}. The barrier in the Ni system appears to be less than that of similar transitions in the other metal systems; the type I and II conformers have largely disappeared at a relatively low temperature (350 K, Figure 3b). Presumably, the d^8 Ni^{2+} electron configuration cannot effectively stabilize the compact I and II states. In solution this ion is often found in square planar geometries,[38] which might also explain the intense type VI conformation observed at 390 K. A larger barrier is associated with the transition between compact type I, II, and III and very open type IV, V, and VI conformations. The activation barrier (<5 kcal mol^{-1}) shown comes from the I,II → IV transition determined from the Ca data. The transition between these groups varies substantially for different metal systems. The data in Figure 3 show that the nickel system unfolds most readily to open conformations. This suggests that the barrier between these two groups is lowest for Ni. At 390 K the $[ICA\text{-}6H + Zn^{2+}]^{4-}$ ion favors a type III conformation, suggesting that the barrier between compact and open conformers is largest in this system.

Conclusions

High-resolution ion mobility techniques have been used to examine the influence of metal binding and source temperature on the conformations of insulin chain A anions in the gas phase. The results indicate that M^{2+} metals bind in specific configurations leading to an overall stabilization of some compact conformations. Compact states are not observed for non-metalated or sodiated peptides having the same net charge (−4). These variations (among non-metalated, sodiated, and M^{2+}−peptide ions) presumably arise because M^{2+} ions are capable of establishing specific M−L binding interactions with various ligands on peptide ($-COO^-$, $-SO_3^-$, and amide groups). These stabilizing interactions result in a broad distribution of different states; 6−10 have been resolved for each of the M^{2+}-systems. Studies as a function of source temperature show that the stabilization of specific conformations is highly mediated by the metal. Presumably, this is a result of differences in specific M−L interactions for different metal ions. Qualitative potential energy surfaces showing the stabilization of compact-metalated states relative to non-metalated conformers have been presented to explain the results. Although we have shown that many conformers can be stabilized and that similarities and differences between states exist, little is understood about the structural details of folded and unfolded states. In particular, the specific interactions of the metal ion with different ligands have not been addressed, due to the tremendously challenging nature of reliable calculations for such systems. In future studies we hope to address the details of M−L interactions that are associated with stabilizing specific conformations in more detail.

Acknowledgment. This work was supported by the National Science Foundation (grant no. CHE-9625199) with additional support from the Petroleum Research Fund administered by the ACS (grant no ACS-PRF 31859-G4). The authors acknowledge Anne E. Counterman for her insight and comments on this paper.

References and Notes

(1) See, for example: Holm, R. H.; Kennepohl, P.; Solomon, E. I. *Chem. Rev.* **1996**, *96*, 2239−2314, and references therein.

(2) Fenn, J. B.; Mann, M.; Meng, C. K.; Wong, S. F.; Whitehouse, C. M. *Science* **1989**, *246*, 64−71.

(3) Karas, M.; Hillenkamp, F. *Anal. Chem.* **1988**, *60*, 2299−2301. Tanaka, K.; Waki, H.; Ido, Y.; Akita, S.; Yoshida, Y.; Yoshida, T. *Rapid Commun. Mass Spectrom.* **1988**, *2*, 151−153.

(4) (a) Mallis, L. M.; Russell, D. H. *Anal. Chem.* **1986**, *58*, 1076−1080. (b) Grese, R. P.; Cerny, R. L.; Gross, M. L. *J. Am. Chem. Soc.* **1989**, *111*, 2835−2842. (c) Zhao, H.; Reiter, A.; Teesch, L. M.; Adams, J. *J. Am. Chem. Soc.* **1993**, *115*, 2854−2863. (d) Hu, P.; Gross, M. L. *J. Am. Chem. Soc.* **1993**, *115*, 8821−8828. (e) Reiter, A.; Adams, J.; Zhao, H. *J. Am. Chem. Soc.* **1994**, *116*, 7827−7838. (f) Loo, J. A.; Peifeng, H.; Smith, R. D. *J. Am. Soc. Mass Spectrom.* **1994**, *5*, 959−965. (g) Hu, P.; Loo, J. A. *J. Am. Chem. Soc.* **1995**, *117*, 11314-11319. (h) Hu, P.; Sorensen, C.; Gross, M. L. *J. Am. Soc. Mass Spectrom.* **1995**, *6*, 1079−1085. (i) Nemirovskiy, O. V.; Gross, M. L. *J. Am. Soc. Mass Spectrom.* **1998**, *9*, 1285−1292.

(5) Tomer, K. B.; Gross, M. L.; Deinzer, M. L. *Anal. Chem.* **1986**, *58*, 2527−2534. Mallis, L. M.; Raushel, F. M.; Russell, D. H. *Anal. Chem.* **1987**, *59*, 980−984. Wu, Q.; Cheng, X.; Hofstadler, S. A.; Smith, R. D. *J. Mass Spectrom.* **1996**, *31*, 669−675. Rodgers, M. T.; Campbell, S. A.; Beauchamp, J. L. *Int. J. Mass. Spectrom. Ion Processes* **1997**, *161*, 193−216.

(6) Penn, S. G.; Cancilla, M. T.; Lebrilla, C. B. *Anal. Chem.* **1996**, *68*, 2331−2339. Cancilla, M. T.; Penn, S. G.; Carroll, J. A.; Lebrilla, C. B. *J. Am. Chem. Soc.* **1996**, *118*, 6736−6745. Cancilla, M. T.; Wong, A. W.; Voss, L. R.; Lebrilla, C. B. *Anal. Chem.* **1999**, *71*, 3206−3218.

(7) Gaucher, S. P.; Leary, J. A. *Anal. Chem.* **1998**, *70*, 3009−3014. Desaire, H.; Leary, J. A. *Anal. Chem.* **1998**, *70*, 1997−2002.

(8) Loo, J. A.; Edmonds, C. G.; Smith, R. D. *Science* **1990**, *248*, 201−204. Wu, Q.; Van Orden, S.; Cheng, X.; Bakhtiar, R.; Smith, R. D. *Anal. Chem.* **1995**, *67*, 2498−2509. Zubarev, R. A.; Kelleher, N. L.; McLafferty, F. W. *J. Am. Chem. Soc.* **1998**, *120*, 3265−3266.

(9) Wyttenbach, T.; von Helden, G.; Bowers, M. T. *Int. J. Mass Spectrom. Ion Processes* **1997**, *165/166*, 377−390.

(10) Gidden, J.; Wyttenbach, T.; Batka, J. J.; Weis, P.; Jackson, A. T.; Scrivens, J. H.; Bowers, M. T. *J. Am. Chem. Soc.* **1999**, *121*, 1421−1422.

(11) Lee, S.; Wyttenbach, T.; Bowers, M. T. *Int. J. Mass Spectrom. Ion Processes* **1997**, *167/168*, 605−614.

(12) Wyttenbach, T.; von Helden, G.; Bowers, M. T. *J. Am. Chem. Soc.* **1996**, *118*, 8355−8364. Wyttenbach, T.; Bushnell, J. E.; Bowers, M. T. *J. Am. Chem. Soc.* **1998**, *120*, 5098−5103.

(13) Wu, C.; Klasmeier, J.; Hill, H. H. *Rapid Commun. Mass Spectrom.* **1999**, *13*, 1138−1142.

(14) Ion mobility spectrometry methods are discussed in the following references: (a) Hagen, D. F. *Anal. Chem.* **1979**, *51*, 870−874. (b) Tou, J. C.; Boggs, G. U. *Anal. Chem.* **1976**, *48*, 1351−1357. (c) Karpas, Z.; Cohen, M. J.; Stimac, R. M.; Wernlund, R. F. *Int. J. Mass Spectrom. Ion Processes* **1986**, *83*, 153−159. (d) St. Louis, R. H.; Hill, H. H. *Crit. Rev. Anal. Chem.* **1990**, *21*, 321−355. (e) von Helden, G.; Hsu, M. T.; Kemper, P. R.; Bowers, M. T. *J. Chem. Phys.* **1991**, *95*, 3835−3837. (f) Jarrold, M. F. *J. Phys. Chem.* **1995**, *99*, 11−21.

(15) For recent reviews of ion mobility studies of biomolecules see: Clemmer, D. E.; Jarrold, M. F. *J. Mass Spectrom.* **1997**, *32*, 577−592. Liu, Y. Valentine, S. J.; Counterman, A. E.; Hoaglund, C. S.; Clemmer, D. E. *Anal. Chem.* **1997**, *69*, 728A−735A. Jarrold, M. F. *Acc. Chem. Res.* **1999**, *32*, 360−367. Hoaglund-Hyzer, C. S.; Counterman, A. E.; Clemmer, D. E. *Chem. Rev.* **1999**, *99*, 3037−3080.

(16) (a) Clemmer, D. E.; Hudgins, R. R.; Jarrold, M. F. *J. Am. Chem. Soc.* **1995**, *117*, 10141−10142. (b) Shelimov, K. B.; Clemmer, D. E.; Hudgins, R. R.; Jarrold, M. F. *J. Am. Chem. Soc.* **1997**, *119*, 2240−2248. (c) Shelimov, K. B.; Jarrold, M. F. *J. Am. Chem. Soc.* **1997**, *119*, 2987−2994.

(17) (a) Valentine, S. J.; Clemmer, D. E. *J. Am. Chem. Soc.* **1997**, *119*, 3558−3566. (b) Valentine, S. J.; Anderson, J.; Ellington, A. E.; Clemmer, D. E. *J. Phys. Chem. B* **1997**, *101*, 3891−3900. (c) Valentine, S. J.; Counterman, A. E.; Clemmer, D. E. *J. Am. Soc. Mass Spectrom.* **1997**, *8*, 954−961.

(18) (a) Covey, T. R.; Douglas, D. J. *J. Am. Soc. Mass Spectrom.* **1993**, *4*, 616−623. (b) Cox, K. A.; Julian, R. K.; Cooks, R. G.; Kaiser, R. E. *J. Am. Soc. Mass Spectrom.* **1994**, *5*, 127−136. (c) Chen, Y. L.; Collings, B.

A.; Douglas, D. J. *J. Am. Soc. Mass Spectrom.* **1997**, *8*, 681−687. (d) Collings, B. A.; Douglas, D. J. *J. Am. Chem. Soc.* **1996**, *118*, 4488−4489.

(19) Kaltashov, I. A.; Fenselau, C. C. *J. Am. Chem. Soc.* **1995**, *117*, 9906−9910. Adams, J.; Strobel, F.; Reiter, A. *J. Am. Soc. Mass Spectrom.* **1996**, *7*, 30−41. Kaltashov, I. A.; Fenselau, C. C. *Proteins* **1997**, *27*, 165−170.

(20) Sullivan, P. A.; Axelsson, J.; Altmann, S.; Quist, A. P.; Sundqvist, B. U. R.; Reimann, C. T. *J. Am. Soc. Mass Spectrom.* **1996**, *7*, 329−341.

(21) Gross, D. S.; Schnier, P. D.; Rodriguez-Cruz, S. E.; Fagerquist, C. K.; Williams, E. R. *Proc. Natl. Acad. Sci. U.S.A.* **1996**, *93*, 3143−3148.

(22) Cassady, C. J.; Carr, S. R. *J. Mass Spectrom.* **1996**, *31*, 247−254.

(23) Winter, B. E.; Light-Wahl, K. J.; Rockwood, A. L.; Smith, R. D. *J. Am. Chem. Soc.* **1992**, *114*, 5897−5898. Suckau, D.; Shi, Y.; Beu, S. C.; Senko, M. W.; Quinn, J. P.; Wampler, F. M.; McLafferty, F. W. *Proc. Natl. Acad. Sci. U.S.A.* **1993**, *90*, 790−793.

(24) Freitas, M.; Marshall, A. G. *Int. J. Mass Spectrom. Ion Processes* **1999**, *182/183*, 221−231.

(25) Schnier, P. D.; Gross, D. S.; Williams, E. R. *J. Am. Chem. Soc.* **1995**, *117*, 6747−6757. Williams, E. R. *J. Mass Spectrom.* **1996**, *31*, 831−842.

(26) Rodriguez-Cruz, S. E.; Klassen, J. S.; Williams, E. R. *J. Am. Soc. Mass Spectrom.* **1997**, *8*, 565−568.

(27) Fye, J. L.; Woenckhaus, J.; Jarrold, M. F. *J. Am. Chem. Soc.* **1998**, *120*, 1327−1328.

(28) Schaaf, T. G.; Stephenson, J. L.; McLuckey, S. A. *J. Am. Chem. Soc.* **1999**, *121*, 8907−8919.

(29) Li, J.; Taraszka, J. A.; Counterman, A. E.; Clemmer, D. E. *Int. J. Mass Spectrom.* **1999**, *185/186/187*, 37−47.

(30) Insight II; Biosym/MSI: San Diego, CA 1995.

(31) Mesleh, M. F.; Hunter, J. M.; Shvartsburg, A. A.; Schatz, G. C.; Jarrold, M. F. *J. Phys. Chem.* **1996**, *100*, 16082−16086. Shvartsburg, A. A.; Jarrold, M. F. *Chem. Phys. Lett.* **1996**, *261*, 86−91.

(32) Counterman, A. E.; Valentine, S. J.; Srebalus, C. A.; Henderson, S. C.; Hoaglund, C. S.; Clemmer, D. E. *J. Am. Soc. Mass Spectrom.* **1998**, *9*, 743−759.

(33) Lee, S. W.; Beauchamp, J. L. *J. Am. Soc. Mass. Spectrom.* **1999**, *10*, 347−351. Hudgins, R. R.; Jarrold, M. F. *J. Am. Chem. Soc.* **1999**, *121*, 3494−3501.

(34) Mason, E. A.; McDaniel, E. W. *Transport Properties of Ions in Gases*; Wiley: New York, 1988.

(35) Jarrold, M. F.; Constant, V. A. *Phys. Rev. Lett.* **1991**, *67*, 2994−2997. Jarrold, M. F.; Honea, E. C. *J. Phys. Chem.* **1991**, *95*, 9181−9185.

(36) This estimation is made by using Poiseuille's law, which assumes laminar flow. See: Harris, W. E.; Habgood, H. W. *Programmed Temperature Gas Chromatography*; Wiley: New York, 1966; pp 23−25.

(37) Activation energies were obtained from linear fits to Arrhenius plots. We note that the data appear to be largely linear over the range studied. However, only a few data points are present in each of the plots; thus, these values are best viewed as estimates.

(38) Cotton, F. A.; Wilkinson, G.; Gaus, P. L. *Basic Inorganic Chemistry*, 3rd ed.; Wiley: New York, 1995.